April 1997

Characterization of Monoped Equilibrium Gaits

William J. Schwind
University of Michigan

Daniel E. Koditschek
University of Pennsylvania, kod@seas.upenn.edu

Characterization of Monoped Equilibrium Gaits

Abstract

We characterize equilibrium gaits of a small knee monoped in terms of manifest parameters by recourse to approximate closed form expressions. We first eliminate gravity during stance and choose a very special model of potential energy storage in the knee. Next, we introduce simple closed form approximations, motivated by the mean value theorem, to the elliptic integrals arising in the more general case. In so doing, we derive a conjectured generalization applicable to small knee monopeds with an arbitrary knee potential. Finally, we introduce a new closed form perturbation intended to adjust the approximate coordinate transformations to the presence of gravity. Simulation data is offered as evidence for the efficacy (to within roughly 5-10% accuracy) of both the proposed generalization across knee potentials and the proposed perturbation for the presence of gravity during stance.

Comments

NOTE: At the time of publication, author Daniel Koditschek was affiliated with the University of Michigan. Currently, he is a faculty member in the Department of Electrical and Systems Engineering at the University of Pennsylvania.

Proceedings of the 1997 IEEE
International Conference on Robotics and Automation
Albuquerque, New Mexico - April 1997

Characterization of Monoped Equilibrium Gaits

William J. Schwind* and Daniel E. Koditschek†
Department of Electrical Engineering and Computer Science
The University of Michigan
Ann Arbor, MI 48109-2110, USA

Abstract

In this paper we characterize equilibrium gaits of a small knee monoped in terms of manifest parameters by recourse to approximate closed form expressions. We first eliminate gravity during stance and choose a very special model of potential energy storage in the knee. Next, we introduce simple closed form approximations, motivated by the Mean Value Theorem, to the elliptic integrals arising in the more general case. In so doing, we derive a conjectured generalization applicable to small knee monopeds with an arbitrary knee potential. Finally, we introduce a new closed form perturbation intended to adjust the approximate coordinate transformations to the presence of gravity. Simulation data is offered as evidence for the efficacy (to within roughly $5-10\%$ accuracy) of both the proposed generalization across knee potentials and the proposed perturbation for the presence of gravity during stance.

1 Introduction

In this paper we pursue a line of inquiry [12, 17] originally stimulated by Raibert's running machines [15]. In our view, the importance of this landmark scientific accomplishment has expanded significantly in the last decade for at least two different reasons. First, from the practical point of view, other robotics researchers, notably, Buehler [14, 10, 1], have developed working variants on these ideas that may be implemented with conventional actuators and onboard power supplies. Second, a growing biomechanics literature suggests the relevance of Raibert's concepts to the understanding of animal gaits [6, 3, 7, 8, 9].

The scope and contributions of this paper may be summarized as follows. Figure 1 (a) depicts the simplest of runners — a lossless two degree of freedom revolute-revolute leg with a massless free (unactuated) ankle, $\overline{q}_{\theta_1}$, and a massless springy knee, $\overline{q}_{\theta_2}$ — that we will call the "spring loaded small knee" (SLSK) monoped.[1] The behavior of any such mechanism, whether engineered or biological, that locomotes in a symmetric equilibrium

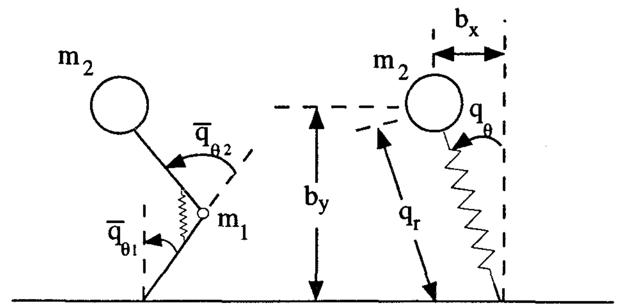

Figure 1: (a) The spring loaded small knee (SLSK) monoped (shown on the left): $1 = m_2 >> m_1 \approx 0$. (b) When $m_1 = 0$ the the SLSK monoped is dynamically equivalent to the spring loaded inverted pendulum (SLIP) monoped (shown on the right).

gait, can be characterized by three parameters that exhaust the possible variations in such motion. We provide closed form expressions that approximate (to within roughly five to ten percent accuracy) the relationship between "internal" and "manifest" triples of these gait description parameters. For example, in Figure 2 we display four different symmetric equilibrium trajectories of the SLSK center of mass (the foot is placed at the origin for the stance portion of each trajectory) where we have systematically varied the duty factor while keeping fixed the height and speed at apex. The "internal" gait description parameters that yield trajectories with these precise properties are computed by solving numerically a set of closed form equations involving familiar transcendental functions that arise from our approximations. Absent our formulae, such an accurately coordinated path through this runner's possible gaits would require a process of repeated numerical integrations from incrementally improved initial conditions.

1.1 Scope of the Paper: Symmetric Equilibrium Gaits

Here and in the sequel, the term gait refers not to the pattern of leg movements of a locomotor, but rather to the trajectory of its center of mass (COM).[2] The distinction is important in general, but for the particular case (the SLSK monoped) considered in this paper, the two notions coincide: there is a change of coordinates — an isometry [18], in fact — between the COM and the leg motions. In point of fact, we will find it most convenient

*Supported in part by a National Science Foundation Graduate Research Fellowship and National Science Foundation Grant IRI-9612357

†Supported in part by National Science Foundation Grant IRI-9510673

[1] The Oxford English Dictionary lists monopode, a usage common in the biomechanics community [7] as a synonym for monoped. We employ the latter since its multileg analogues are more familiar than, for instance, bipode or quadrapode, etc.

[2] While the first notion of gait may be more familiar, both notions appear in the literature [2, 4, 9].

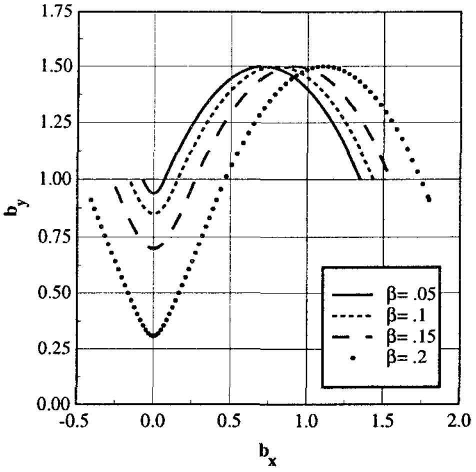

Figure 2: Trajectory of COM over one cycle (for compressed air spring model with no gravity during stance) holding constant both the horizontal velocity, $\dot{\bar{b}}_x = 2m/s$, and height at apex, $\bar{b}_y = 1.5m$, while adjusting duty factor (% time in flight) between 5% and 20% in uniform increments. In each case the foot is placed at the origin during the stance phase and the flight phase begins when b_y crosses for a second time its initial value.

to work in a different coordinate system altogether. Letting $m_1/m_2 \to 0$, as the SLSK model assumes, yields an isometry to polar coordinates. [3]

Thus, throughout the remainder of the paper, we will express most of our results in these revolute-prismatic coordinates.

Say that a motion [4] is an *equilibrium gait* if the trajectory resulting from a set of leg placements is identical to the previous trajectory for the same set of leg placements. In other words, the equilibrium gaits are periodic orbits of the locomotor dynamics, and we may identify such trajectories with the fixed points of an associated "return map" [12, 19, 16]. What we have called the internal gait description parameters comprise a point on a transverse section (the leg compression, r_b, and the angular velocity of the mass relative to the fixed ankle at the bottom of the stance phase, ω_b) together with a control parameter (the spring constant, k) to form the triple that we denote $p_b = (r_b, \omega_b, k) \in \mathcal{P}_b$. Thus, our transformations back to such manifest parameters as the apex properties selected in Figure 2 amount to computing explicitly a component of the return map of the locomotor dynamics.

Our use of the word symmetry formalizes Raibert's notion of *neutral orbits.* These are joint space motions that are even or odd as time functions considered with respect to an origin defined by the bottom of the stance phase. For now, the reader may simply imagine requiring the second half of the stance phase to mirror the first half. These ideas are briefly explored in Section 2.3.1, although a more formal exposition is found in [18].

Unfortunately, such a mathematically natural view of these gait description parameters is unsatisfactory. From the robotics point of view, they do not coincide with the available control inputs. The spring constant is in plain sight, but the effect of leg angle at touchdown is obscured. From a biomechanician's point of view, they do not correspond to external observables that would be straightforward to measure in an intact animal, notwithstanding the experimental ingenuity of such researchers as Full, McMahon and colleagues, who have reported the ability to extract estimates for the SLIP model spring constant for a variety of animals [7, 8]. In either case, one desires a transparent means of relating the mathematically convenient "internal" parameters to such "manifest" properties as we display in Figure 2. But the mathematics relating these properties seems on the face of it intractable. Specifically, the dynamics take the general form of the "restricted three body problem" from classical mechanics [5]. Thus, this simplest of locomotion systems is not merely nonintegrable but its motions may be expected to exhibit the formidably intricate patterns that launched Poincaré on his study of what has since come to be called "chaos" [11].

1.2 Contribution of the Paper: From Internal to Manifest Gait Description Parameters

Recourse to numerical integration is of course unimaginably advanced relative to Poincaré's time, and the question naturally arises why any more need be said. In answer, for the applications we envision, one seeks a functional means of relating manifest effects to internal causes whereby the various physical influences that achieve or perturb the desired patterns are subject to reasoned deductions rather than trial and error computation. The precisely tuned orbits of Figure 2 presents a typical example. Thus, our problem in this paper is to provide some means of characterizing these equilibrium gaits in terms of manifest parameters and to do so by recourse to closed form expressions. Our solution to this problem may be summarized as follows.

We first eliminate gravity during stance and choose a very special model of potential energy storage in the knee, in Section 3. This particular spring law is not a mere mathematical curiosity since it provides a simplistic but not unreasonable model of the compressed air spring that Raibert has used in many of his robots [15, 16]. Moreover, we have gained significant understanding of Raibert's control policies in the past by removing the effects of gravity during stance as well [12, 17]. These simplifications afford a carefully structured instance of the system that can be integrated in terms of elementary functions using techniques dating back to the origins of classical mechanics [20]. We manipulate these expressions to obtain functional relationships between the internal gait description parameters and the manifest apex parameters.

Next, in Section 4, we introduce simple closed form approximations, motivated by the Mean Value Theorem, to the elliptic integrals arising in the more general case. In so doing, we derive a conjectured generalization applicable to small knee monopeds with an arbitrary knee

[3] To be exact, the isometry breaks at the critical points (straight leg and doubled over leg) reflecting the fact that the torus is a double cover of the punctured disk [18]. It should be intuitively clear, however, that monoped legs will not operate anywhere near these critical points.

[4] We will adopt the terminology of dynamical systems theory and use *motion, trajectory, orbit,* synonymously to denote the solution in time of the leg dynamics from a particular initial condition.

potential, still in the absence of gravity during stance (13). We test this spring law generalization by choosing a very different knee potential — the linear-in-extension (Hook's law) spring — motivated by the physical models that Buehler has used in describing his machines [14, 10]. While the equations of motion for this knee are still integrable in the formal mathematical sense, the elliptic integrals that result are almost as opaque to the kind of parametric insight one desires as the original Runge-Kutta simulations. We present detailed numerical evidence verifying the correspondence of the closed form but approximate coordinate transformation to the exact mathematical relationships given by these elliptic integrals. In a longer report [18] we present similarly detailed numerical evidence establishing the surprising accuracy of these approximation formulae for a much broader range of physically plausible knee potentials.

Finally, in Section 5, we introduce a new closed form perturbation intended to adjust the approximate coordinate transformations to the presence of gravity. Once again, we present detailed numerical evidence suggesting the very good fit between our closed form expression (13) and the full, nonintegrable "chaotic" truth.

A concluding section suggests the immediate applications and more distant implications of these three contributions.

2 Symmetric Equilibrium Gaits of the SLIP Monoped

In this section we re-interpret the questions of interest concerning the SLSK monoped in terms of the equivalent SLIP model, and then go on to develop the formal properties of the latter that will be exploited to derive our results.

2.1 Potential Energy

It will be important in the sequel to develop our results in a form that is valid across a large family of spring models for the locomotor's knee. This degree of generality is required because it seems clear that the most appropriate model of potential energy may well vary over the intended application of interest.

While virtually all successful legged robots to date have adopted the revolute prismatic kinematics of the SLIP monoped, biomechanicians have heretofore adopted this model [7] only in analogy to the more biologically valid revolute-revolute kinematics. We introduce the SLSK version of the revolute-revolute design with the hope of trimming the gap between physical analogy and fact. Thus, we are greatly concerned to insure that all insights developed for one model apply to both. The models will be dynamically equivalent if and only if their spring forces are related through the transposed jacobian of the isometry, $g^{-1} \circ \overline{g}$ [18]. Thus, while it is straightforward to express a given spring law in one or another set of coordinates, it is equally clear that simple expressions in one set will yield very complex expressions in the other, and vice versa. In other words, simplistic models of the knee potential will have very different properties depending upon whether we are using them to capture "elements" of reality pertaining to the SLSK or the SLIP leg.

Gait Description Parameters	
k	Spring Constant
(r_b, ω_b)	Leg Length and Angular Vel. at Bottom
$(q_{rl}, q_{\theta l})$	Leg Length and Angle at Lift-Off
$(\dot{q}_{rl}, \dot{q}_{\theta l})$	Radial and Angular Vel. at Lift-Off
$(\dot{b}_{xl}, \dot{b}_{yl})$	Forward and Vertical Vel. at Lift-Off
$(\bar{b}_y, \dot{\bar{b}}_x)$	Hopping Height and Forward Vel. at Apex
ϕ	$\frac{TimeFlight}{TimeStance} = \frac{t_f}{t_s}$
β	Duty Factor $= \frac{1}{2(1+\phi)}$

Gait Description Parameters	
p_b	Bottom Gait Parameters (r_b, ω_b, k)
p_l	Polar Lift-Off Gait Param. $(q_{\theta l}, \dot{q}_{rl}, \dot{q}_{\theta l})$
$\overline{p}_m$	Manifest Apex Gait Parameters $\left(b_y, \dot{\bar{b}}_x, \beta\right)$

Gait Description Parameter Spaces	
$\mathcal{P}_b$	Bottom Gait Parameter Space
$\overline{\mathcal{P}}_m$	Manifest Apex Gait Parameter Space

Leg Coordinates	
$\boldsymbol{b}$	Cartesian Pos. Coordinates, $[\, b_x,\ b_y\,]^T$
$\dot{\boldsymbol{b}}$	Cartesian Vel. Coordinates, $[\, \dot{b}_x,\ \dot{b}_y\,]^T$
$T\boldsymbol{b}$	$[\, \boldsymbol{b},\ \dot{\boldsymbol{b}}\,]^T$
$\boldsymbol{q}$	Polar Pos. Coordinates, $[\, q_r,\ q_\theta\,]^T$
$\dot{\boldsymbol{q}}$	Polar Vel. Coordinates $[\, \dot{q}_r,\ \dot{q}_\theta\,]^T$
$T\boldsymbol{q}$	$[\, \boldsymbol{q},\ \dot{\boldsymbol{q}}\,]^T$

Leg Coordinate Maps	
g	Polar to Cartesian Coordinate Map
$D\boldsymbol{q}g$	Polar to Cartesian Velocity Map
Tg	Polar to Cartesian Tangent Map

Table 1: Notation used throughout the paper

We have chosen to explore a family of spring potentials whose appearance is mathematically simple when expressed in the SLIP model. In the more detailed technical report [18], we have worked in the SLIP coordinates with various potential functions of the general "power law" form

$$U_{(i,j)}(q_r, q_{r0}, k) = \frac{k}{|i \cdot j|} P_i(-sgn(j)\,[P_j(q_r) - P_j(q_{r0})])\,; \quad P_l(x) := x^l, l \in I\!N \tag{1}$$

including both the "compressed air spring"

$$U_A(q_r) := U_{(1,-2)}(q_r, q_{r0}, k) = \frac{k}{2}(1/q_r^2 - 1/q_{r0}^2) \tag{2}$$

and the "Hook's law spring"

$$U_H(q_r) := U_{(2,1)}(q_r, q_{r0}, k) = \frac{k}{2}(q_{r0} - q_r)^2, \tag{3}$$

discussed explicitly in the present paper. [5]. As we have remarked above, these latter two are of particular interest from the applications perspective in view of

[5] For $l = 0$ we take $P_0(x) := \ln(x)$.

their "simplistic but not unreasonable" representation of Raibert's and Buehler's SLIP machines, respectively. [6]

As will be seen directly below, the first spring, U_A is a particularly fortuitous choice for mathematical reasons. In point of fact, the motivation for the potential family, (1), is similar in spirit to that of the classical mechanicians. In fact, our family is essentially captured by the ancient catalogue presented by Whittaker [20, Ch.4 §47], but for the (important!) distinction that the celestial central forces are attracting and our locomotor's knee forces are repelling. [7]

With this understanding in force, we now presume a generic spring potential, $U(k, q_r)$, where k is the spring constant q_r is the leg length, and we may proceed with a presentation of the dynamics.

2.2 Locomotor Dynamics

The monoped flies through the air as a two degree of freedom point mass subject to gravity, and then touches down, maintaining a fixed ankle position relative to the ground throughout the stance phase until the rising hip pulls the ankle off the ground and flight begins anew. We assume that the leg angle at touchdown can be freely selected in flight. Newtonian free flight dynamics are readily integrable, so the only point of inquiry concerns the stance dynamics that we now present.

The equations of motion during stance can be derived in any of the three coordinate systems (COM, SLSK, SLIP) discussed above using the traditional Euler-Lagrange formulation. The proper choice of coordinates is, of course, a matter of convenience, since the dynamics expressed in any one coordinate system are identical in behavior (albeit not in appearance) to the others. However, the traditional quadrature formulae for low degree of freedom central force problems have been worked out in the analogues of the SLIP model, and we have found it most convenient to proceed following that model.

More specifically, we have found it easy to formalize Raibert's notion of symmetry in the latter model, and less intuitively informative to do so in the other two coordinate systems. The familiar SLIP dynamics can be found in [18].

2.3 Gait Description Parameters

We now explore the implications of reverse time symmetry in identifying what we have termed the "internal gait description parameters" in the discussions above. We list two collections of physically interesting measureables as examples of "manifest" features that we might wish to relate back to them.

2.3.1 The Symmetry, S, and its Neutral Orbits, $\mathcal{N}$

We have introduced the ideas of reverse time symmetries and neutral orbits in a previous paper [17], and have related them in a substantially similar form in several recent papers, notably [13]. These ideas are also carefully formalized in [18].

The set of fixed points of the SLIP symmetry is given by

$$\text{Fix}S = \{T\boldsymbol{q} \in T\boldsymbol{Q} | q_\theta = 0 \ \& \ \dot{q}_r = 0\}$$

All nontrivial stance motions of a SLIP monoped must pass through a state of maximal spring compression (i.e., where $\dot{q}_r = 0$). This is, in fact, the condition that Raibert used to define his notion of the "bottom" of the stance phase. Clearly, not all stance motions will pass through the bottom condition at the same instant that the leg is perfectly vertical. However, Fix$S$ is exactly the union of such bottom states.

Lemma 2.1, proved in [18], shows that any stance motion whose bottom is vertical in this manner must have the symmetry property that Raibert has identified and exploited to such advantage in his empirical work.

Lemma 2.1 *If the next touchdown angle is chosen to be the negative of the current lift-off angle, i.e.* $q_{\theta t}(n+1) = -q_{\theta l}(n)$*, then any* $T\boldsymbol{q}_b \in$ Fix$S$ *is a fixed point of the bottom return map.*

The two-dimensional manifold Fix$S$ is parameterized by it's values of q_r and $\dot{q}_\theta$, which we henceforth refer to as r_b and ω_b respectively. Given a spring constant, k, any neutral orbit is parameterized by it's values of r_b and ω_b. Since the neutral orbits are in equilibrium as shown in Lemma 2.1, we see that any equilibrium gait is completely characterized by its values of r_b, ω_b and k. This observation leads naturally to an internal gait parameter space given by $p_b = (r_b, \omega_b, k)$. We have already remarked that notwithstanding its mathematical convenience, p_b, is deficient from an applications perspective. Consequently, we introduce a number of other gait parameter spaces, each with it's own utility in applications.

In the spirit of Raibert's work [15], we would like to prescribe a gait using easily measurable and understood quantities such as hopping height, forward velocity and duty factor [8], which we will refer to as the manifest apex parameter space, $\overline{p}_m = (\overline{b}_y, \dot{\overline{b}}_x, \beta)$.

Since we are interested in generating specified gaits, we would like to understand how a particular choice of $\overline{p}_m$ determines $p_l = (q_{\theta l}, \dot{q}_{rl}, \dot{q}_{\theta l})$ and $p_b = (r_b, \omega_b, k)$. Once again, we follow Raibert in using desired hopping height to determine $k \in p_b$ [9], and desired forward velocity to determine $q_{\theta l} \in p_l$ [10].

We would like to understand for a general SLIP model the change of coordinates between each parameter space. In this paper we will concentrate on ${}^{\overline{m}}_{b}\boldsymbol{H}$:

[6] In the former case, k is the natural "control parameter" since Raibert adjusts the air pressure during stance [15]. In the latter case, q_{r0} is the more realistic "control parameter," and properly should replace k in the internal gait description space, $\mathcal{P}_b$, since Buehler drives a small motor that adjusts the spring offset through a wormdrive. Since both parameters enter our formulae, there would be no difficulty in making this substitution in a particular application. However, we choose to stick with k in both models throughout the paper for ease of exposition.

[7] It is fascinating, philosophically speaking, to note that even the simplest of runners must "know" celestial mechanics merely to find an equilibrium.

[8] Raibert's algorithms don't explicitly specify duty factor. However, that parameter is arguably the quantity that coordinates the hopping height and forward velocity into a distinct gait as we try to portray in Figures 2

[9] Raibert's control strategy implements the inverse: k determines hopping height.

[10] Because we are assuming equilibrium gaits, determining the lift-off leg angle is identical to determining the touchdown leg angle.

$p_b \mapsto \overline{p}_m$. However in future work, we would like to focus on the maps ${}^{l}_{m}\boldsymbol{H}$ and ${}^{b}_{m}\boldsymbol{H}$, which are of special interest from a control perspective, since they dictate how a gait specification in terms of $\overline{p}_m$ is transformed into a gait generation in terms of p_l and p_b.

3 Exact Integration of Stance Dynamics

We now introduce simplifications in the SLIP model resulting in closed-form integrable stance dynamics, and by so doing, derive exact closed form expressions for the map ${}^{m}_{b}\boldsymbol{H}$ (we will use non-bold H for the change of coordinates of this special case). The mathematical details of these derivations are given in [18] and we focus here on the larger view of how this is achieved.

3.1 Removing Gravity and Choosing a Special Spring

We begin by eliminating gravity from the stance dynamics. This simplification implies conservation of angular momentum during stance, rendering q_θ a cyclic variable [5] and yielding the relationship, $\frac{d\dot{q}_\theta}{dq_r} = \frac{-2\dot{q}_\theta}{q_r}$. Because we are interested in equilibrium gaits, we choose the initial condition $T\boldsymbol{q}_0 \in \text{Fix}S$. Solving for $\dot{q}_\theta$ we find,

$$\dot{q}_\theta(p_b, q_r) = \omega_b(\frac{r_b}{q_r})^2 \tag{4}$$

Substituting (4) into the conserved total energy allows us to solve for $\dot{q}_r$,

$$\dot{q}_r(p_b, q_r, U) = \left[r_b^4\omega_b^2\left(\frac{1}{r_b^2} - \frac{1}{q_r^2}\right) + 2(U(r_b) - U(q_r))\right]^{\frac{1}{2}}. \tag{5}$$

It should be noted that even though we have assumed $T\boldsymbol{q}_0 \in \text{Fix}S$, the results of (4) and (5) hold for the more generalized notion of bottom condition, where we only require that $\dot{q}_{rb} = 0$ [16].

Since we have now expressed both $\dot{q}_r$ and $\dot{q}_\theta$ as functions of q_r alone, we can exploit the relationship $\frac{dq_\theta}{dq_r} = \frac{\dot{q}_\theta}{\dot{q}_r}$ to solve for q_θ. Integrating, we obtain

$$q_\theta(p_b, q_r, U) \quad = \quad \int_{r_b}^{q_r} \frac{\dot{q}_\theta(p_b, q_r)}{\dot{q}_r(p_b, q_r, U)}\, dq_r \tag{6}$$

The analytical tractability of the above integral depends greatly on the choice of the spring potential $U(q_r)$. The structure of the integral suggests certain forms for the spring law which are physically realistic and also admit closed form integration. We have chosen to work with the compressed air spring, $U_A(q_r)$ given in (2) [16]. Using this new spring law, we find

$$\begin{bmatrix} q_\theta(p_b, q_r) \\ \dot{q}_r(p_b, q_r) \\ \dot{q}_\theta(p_b, q_r) \end{bmatrix} = \begin{bmatrix} -\left[\frac{r_b^4\omega_b^2}{r_b^4\omega_b^2+k}\right]^{\frac{1}{2}} acot\left(\left[\frac{r_b^2}{q_r^2-r_b^2}\right]^{\frac{1}{2}}\right) \\ \left[\left(r_b^4\omega_b^2 + k\right)\left(\frac{1}{r_b^2} - \frac{1}{q_r^2}\right)\right]^{\frac{1}{2}} \\ \omega_b(\frac{r_b}{q_r})^2 \end{bmatrix} \tag{7}$$

3.2 Exact Poincaré Map

Given the exact stance integration (7) we can derive the change of coordinate map ${}^{m}_{b}H$. The general derivation is outlined in Section 4.2, while the particular derivation for the special case under consideration is presented explicitly in [18].

4 General Spring Law Corrections

From a mathematical perspective the introduction in (6) of the compressed air spring (2) is unnecessary. For even without the particular spring law the problem was formally "solved" – we had closed-form solutions for $\dot{q}_r$ and $\dot{q}_\theta$ and we had q_θ as an elliptic integral. However, as engineers, we desire more than just an analytical solution. We hope to gain insight into the role each gait parameter plays in gait generation. In this section we will generalize the results of the previous section to other spring laws by introducing simple closed form approximations, arising from application of the Mean Value Theorem (MVT), for the elliptic integrals $q_{\theta l}$ and t_s. We will offer simulation results as evidence of the validity of the general form of the approximations.

4.1 MVT Approximations

For the no gravity SLIP dynamics with a general spring law, U, the lift-off angle, $q_{\theta l}$ is given by

$$q_{\theta l} \quad = \quad \int_{r_b}^{q_{rl}} \frac{\dot{q}_\theta(p_b, q_r)}{\dot{q}_r(p_b, q_r, U)}\, dq_r = \int_{r_b}^{q_{rl}} i_\theta(p_b, q_r, U)\, dq_r \tag{8}$$

By the MVT, there exists $\xi_{\theta l} \in (r_b, q_{rl})$ and similarly $\xi_{ts} \in (r_b, q_{rl})$ [11], such that

$$q_{\theta l} \;=\; i_\theta(p_b, \xi_{\theta l}, U)\,(q_{rl} - r_b) \tag{9}$$
$$t_s \;=\; 2 i_t(p_b, \xi_{ts}, U)\,(q_{rl} - r_b) \tag{10}$$

Although guaranteeing the existence of $\xi_{\theta l}$ and ξ_{ts}, the MVT does not give an explicit formulation for their calculation. To actually generate the values of $q_{\theta l}$ and t_s we need to explore whether functional relationships of the form $\xi_{\theta l} = f_\xi(p_b, q_{rl}, U, q_{\theta l})$ and $\xi_{ts} = f_\xi(p_b, q_{rl}, U, t_s)$ can be determined.

Two methods for generating approximate functions for $\xi_{\theta l}$ and ξ_{ts} will be discussed. The first method considers the particular case where the elliptic integrals and

[11] In general the value of ξ_{ts} will be different from $\xi_{\theta l}$. However, the ξ introduced in Equation (11) yields good results in both cases.

	Max % Err	Mean % Err	MSE
$q_{\theta l}$	2.49	1.22	6.94×10^{-5}
t_s	4.03	2.60	1.14×10^{-4}

Table 2: Errors, $\| q_{\theta l} - \hat{q}_{\theta li} \|_2$, $\| t_s - \hat{t}_{si} \|_2$, with $\xi_{\theta l}$ and ξ_{ts} given in Equation (11) with $\alpha = \frac{3}{4}$, for the Hook's law spring, $U_H(q_r)$ $\mathcal{D} = [0.45, .95] \times [-1, -10] \times [10, 100] \subseteq \mathcal{P}_b$.

hence the relationships for $\xi_{\theta l}$ and ξ_{ts} can be calculated in closed form, In the second case we assume a linear approximation with slope determined by the asymptotic behavior of $\frac{\partial \xi}{\partial r_b}$ as $r_b \rightarrow q_{rl}$.

4.1.1 Mean Values for $U_A(q_r)$ Spring Law

In Section 3.1, the compressed air spring U_A is selected because it yields closed form solutions for $q_{\theta l}$ (7) and t_s. Given these closed form solutions, we can solve equations (9) and (10) for the exact values of $\xi_{\theta l}$ and ξ_{ts}. A more detailed report [18] documents the results and demonstrates that these exact values for the U_A spring serve as good approximations for a variety of other spring laws including U_H.

4.1.2 Linear Approximation of Mean Values

The simplest functional representation for the mean values, $\xi_{\theta l}$ and ξ_{ts} would be a linear approximation of the form,

$$\xi = \alpha r_b + (1 - \alpha) q_{rl} \tag{11}$$

We have shown [18] that independent of the spring potential for both $\xi_{\theta l}$ and ξ_{ts},

$$\lim_{r_b \rightarrow q_{rl}} \frac{\partial \xi}{\partial r_b} = \frac{3}{4} \tag{12}$$

The analysis suggests setting $\alpha = \frac{3}{4}$ in equation (11). In addition to yielding a good approximation for r_b close to q_{rl}, we also find it to quite be effective over a reasonably large portion of the parameter space. Table 2 displays simulation data for the U_H spring documenting the difference between the real values of $q_{\theta l}$ and t_s and those generated using equations (9) and (10) with the mean value of equation (11). In each case the maximum percent error is less than 4.1%, the mean percent error is less than 2.6% and the mean squared error is less than 1.2×10^{-4}. Similar results are found for a variety of spring laws and are documented in [18].

4.2 Generalized Poincaré Map, ${}^{m}_{b}\hat{\boldsymbol{H}}$

Given these approximations for $q_{\theta l}$ and t_s, we can derive a generalized form of ${}^{m}_{b}\hat{\boldsymbol{H}}$ that can be used for any spring law.

$${}^{m}_{b}\hat{\boldsymbol{H}} = \begin{bmatrix} q_{rl}\cos(q_{\theta l}(p_b, q_{rl}, U)) + \frac{\dot{b}_{yl}(p_b, q_{rl}, U)^2}{2g} \\ \dot{b}_{xl}(p_b, q_{rl}, U) \\ \frac{1}{2\left(1 + \frac{2\dot{b}_{yl}(p_b, q_{rl}, U)}{g t_s(p_b, q_{rl}, U)}\right)} \end{bmatrix} \tag{13}$$

	Max % Err	Mean % Err	MSE
$\overline{p}_m$	1.03	0.38	3.9×10^{-4}
$\overline{b}_x$	1.63	0.31	1.8×10^{-4}
$\overline{b}_y$	3.49	0.82	1.2×10^{-4}
$\overline{\beta}$	13.1	2.12	9.3×10^{-5}

Table 3: Errors, $\| {}^{m}_{b}\boldsymbol{H} - {}^{m}_{b}\hat{\boldsymbol{H}} \|_2$, for the Hook's law spring, $U_H(q_r)$ $\mathcal{D} = [.45, .95] \times [-1, -10] \times [10, 100] \subseteq \mathcal{P}_b$ and $\mathcal{I} \subseteq [0.68, 9.51] \times [0.53, 2.52] \times [0.11, 0.48] \subseteq \overline{\mathcal{P}}_m$.

Where $\dot{b}_l(p_b, q_{rl}, U) = D_{\boldsymbol{q}}g\,\dot{\boldsymbol{q}}_l$; $\dot{\boldsymbol{q}}_l$ is obtained by evaluating (5) and (4) at $q_r = q_{rl}$; and $q_{\theta l}$ and t_s are obtained by evaluating (9) and (10) at ξ given by (11).

We now have ${}^{m}_{b}\hat{\boldsymbol{H}}$ in equation 13 in terms of quantities that we know for each spring law. As evidence for the validity of ${}^{m}_{b}\hat{\boldsymbol{H}}$, we offer simulation data for the U_H spring law. The data in table 3 compares the results of ${}^{m}_{b}\boldsymbol{H}$ and ${}^{m}_{b}\hat{\boldsymbol{H}}$ for the U_H spring law over a given set of p_b (the domain of p_b explored in the simulations and the resulting bound on the image of p_m are documented in the table captions). It shows the maximum percent error, mean percent error and mean squared error for the vector $\overline{p}_m$ as a whole and also for each component individually. In this case all the mean percent errors are less than 2.2% and the mean squared errors are all less than 4.0×10^{-4}.

Simulation data for other spring laws are presented in [18] and are found to have errors that are very similar to those of Table 3.

5 Gravity Corrections

All of the formulae derived so far ignore gravity during the stance phase. We now reconsider the perturbed system, where gravity is re-introduced to the stance phase.

In the "no gravity" case, the only potential energy is that stored in the spring. In the perturbed system there is both spring and gravitational potential energy. Consider temporarily that the monoped is restricted to purely vertical motion and consider the spring potential at bottom. We would want the spring potential of the perturbed system at bottom, $U_g(r_b)$ to be greater than the spring potential at bottom of the unperturbed system, $U(r_b)$ by the amount of the gravitational potential the leg will have to overcome traveling from bottom to lift-off, $g(q_{rl} - r_b)$. That is, we want

$$U_g(r_b) - U(r_b) = g(q_{rl} - r_b) \tag{14}$$

This insight is used to generate a simple, yet effective function, $\boldsymbol{P} : \mathcal{P}^g_b \mapsto \mathcal{P}_b$, such that

$${}^{m}_{b}\hat{\boldsymbol{H}}_g(p^g_b) = {}^{m}_{b}\hat{\boldsymbol{H}} \circ \boldsymbol{P}(p^g_b) \tag{15}$$

In particular, we choose $\boldsymbol{P}$ to introduce a translation in the spring constant component via the relationship presented in (14).

For the case of the compressed air spring, $U_A(q_r)$, this yields,

$$\boldsymbol{P}(p^g_b) = \begin{bmatrix} r_b \\ \omega_b \\ k_g - \frac{2g q_{rl}^2 r_b^2}{q_{rl} + r_b} \end{bmatrix} \tag{16}$$

	Max % Err	Mean % Err	MSE
p_m	25.2	6.15	0.09
$\bar{b}_x$	27.5	6.63	0.086
$\bar{b}_y$	13.7	3.47	1.6×10^{-3}
β	37.9	13.4	2.6×10^{-3}

Table 4: Errors, $\| \,{}^m_b\boldsymbol{H}_g - {}^m_b\hat{\boldsymbol{H}}_g \|_2$, for the Hook's law spring, $U_H(q_r)$ with gravity compensation $\mathcal{D} = [0.45, .95] \times [-1, -10] \times [45.6, 492] \subseteq \mathcal{P}_b$ and $\mathcal{I} \subseteq [0.75, 9.56] \times [0.58, 2.53] \times [0.10, 0.42] \subseteq \mathcal{P}_m$.

The data in Table 4 compares the results of ${}^m_b\boldsymbol{H}_g$ and ${}^m_b\hat{\boldsymbol{H}}_g$ for a given set of p_b for the $U_H(q_r)$ spring law. It shows the maximum percent error, mean percent error and mean squared error for the vector p_m as a whole and also for each component individually. In each case the mean percent error is roughly $5-10\%$ and the mean squared error is less than .09.

While the errors are much larger than those of Table 3, they are still very reasonable and in any case the size of the errors introduced must be weighed against the benefit of having the closed form functional approximation, ${}^m_b\hat{\boldsymbol{H}}_g$, for cases which are otherwise not closed form integrable.

6 Conclusion

We believe that there are three distinct audiences for the work presented in this paper. Most obviously, in the engineering community, we hope that our approximations will make it easier for programmers of both animated simulations and physical locomotion machines to select and achieve more precise legged behavior. Similarly, we hope that biomechanicians may find the general pattern of relationships between internal and manifest gait description parameters helpful in designing more focussed experiments to pin down the validity of detailed mathematical models of biological behavior. Finally, we suspect that applied mathematicians may be intrigued by both the success of our mean value approximations and the success of our relatively simple perturbation formulae in place of the much more complicated expressions likely to result from a formal perturbation analysis of the integrable system.

Acknowledgements

We thank Profs. Anthony Bloch and Phillip Holmes for a number of informative tutorial discussions bearing on the problems addressed in this paper. We thank Patrick Hagerty for a number of stimulating discussions as well.

References

[1] M. Ahmadi and M. Buehler. Stable control of a simulated one-legged running robot with hip and leg compliance. *IEEE Transactions on Robotics and Automation*, 1996. To Appear.

[2] R. M. Alexander. The gaits of bipedal and quadrapedal animals. *International Journal of Robotics Research*, 3(2):49–59, 1984.

[3] R. M. Alexander. Three uses for springs in legged locomotion. *International Journal of Robotics Research*, 9(2):53–61, 1990.

[4] R. M. Alexander and A. S. Jayes. Vertical movement in walking and running. *Journal of Zoology, London*, 185:27–40, 1978.

[5] V. I. Arnold. *Mathematical Methods of Classical Mechanics.* Springer-Verlag, New York, 1978.

[6] R. Blickhan. The spring-mass model for running and hopping. *Journal of Biomechanics*, 22:1217–1227, 1989.

[7] R. Blickhan and R. J. Full. Similarity in multilegged locomotion: Bouncing like a monopode. *Journal of Comparative Physiology*, 173:509–517, 1993.

[8] C. T. Farley, J. Glasheen, and T. A. McMahon. Running springs: Speed and animal size. *Journal of Experimental Biology*, 185:71–86, 1993.

[9] R. J. Full. Integration of individual leg dynamics with whole body movement in arthropod locomotion. In R. D. Beer, R. E. Ritzmann, and T. McKenna, editors, *Biological Neural Networks in Invertebrate Neuroethology and Robotics*, pages 3 -20. AP, San Diego, CA, 1993.

[10] P. Gregorio, M. Ahmadi, and M. Buehler. Experiments with an electrically actuated planar hopping robot. In T. Yoshikawa and F. Miyazaki, editors, *"Experiemental Robotics III," Lecture Notes in Control and Information Sciences 200*, pages 269–281. Springer, 1994.

[11] P. Holmes. Poincaré, celestial mechanics, dynamical systems theory and "chaos". *Physics Reports (Review Section of Physics Letters)*, 193(3):137–163, 1990.

[12] D. E. Koditschek and M. Bühler. Analysis of a simplified hopping robot. *International Journal of Robotics Research*, 10(6):587–605, December 1991.

[13] J. Nakanishi, T. Fukuda, and D. E. Koditschek. Preliminary studies of robot brachiation. In *Proceedings of the IEEE International Conference On Robotics and Automation*, 1997.

[14] H. Rad, P. Gregorio, and M. Buehler. Design, modeling and control of a hopping robot. In *Proceedings of the IEEE/RSJ Conference On Intelligent Systems and Robots*, pages 1778–1785, Yokohama, Japan, July 1993.

[15] M. H. Raibert. *Legged Robots That Balance.* MIT Press, Cambridge, MA, 1986.

[16] W. J. Schwind and D. E. Koditschek. Control of forward velocity for a simplified planar hopping robot. Technical Report CGR-94-12, Department of Electrical Engineering and Computer Science, University of Michigan, 1994.

[17] W. J. Schwind and D. E. Koditschek. Control of forward velocity for a simplified planar hopping robot. In *Proceedings of the IEEE International Conference On Robotics and Automation*, Nagoya, Japan, May 1995.

[18] W. J. Schwind and D. E. Koditschek. Characterization of monoped equilibrium gaits. Technical report, Department of Electrical Engineering and Computer Science, University of Michigan, 1997.

[19] A. F. Vakakis, J. W. Burdick, and T. K. Caughy. An 'interesting' strange attractor in the dynamics of a hopping robot. *International Journal of Robotics Research*, 10(6):606–618, December 1991.

[20] E. T. Whittaker. *A Treatise on the Analytical Dynamics of Particles and Rigid Bodies.* Cambridge University Press, New York, fourth edition, 1904.